

Journal of Turbulence

Publication details, including instructions for authors and
subscription information:

<http://www.tandfonline.com/loi/tjot20>

The signature of laminar instabilities in the zone of transition to turbulence

N. Vinod^a & R. Govindarajan^a

^a Engineering Mechanics Unit, Jawaharlal Nehru Centre for
Advanced Scientific Research, Jakkur, Bangalore, 560 064, India

Available online: 02 Nov 2009

To cite this article: N. Vinod & R. Govindarajan (2007): The signature of laminar instabilities in the
zone of transition to turbulence, Journal of Turbulence, 8, N2

To link to this article: <http://dx.doi.org/10.1080/14685240600851732>

PLEASE SCROLL DOWN FOR ARTICLE

Full terms and conditions of use: <http://www.tandfonline.com/page/terms-and-conditions>

This article may be used for research, teaching, and private study purposes. Any
substantial or systematic reproduction, redistribution, reselling, loan, sub-licensing,
systematic supply, or distribution in any form to anyone is expressly forbidden.

The publisher does not give any warranty express or implied or make any representation
that the contents will be complete or accurate or up to date. The accuracy of any
instructions, formulae, and drug doses should be independently verified with primary
sources. The publisher shall not be liable for any loss, actions, claims, proceedings,
demand, or costs or damages whatsoever or howsoever caused arising directly or
indirectly in connection with or arising out of the use of this material.

The signature of laminar instabilities in the zone of transition to turbulence

N. VINOD* and R. GOVINDARAJAN*

Engineering Mechanics Unit, Jawaharlal Nehru Centre for Advanced Scientific Research,
Jakkur, Bangalore 560 064, India

We demonstrate that the spacetime statistics of the birth of turbulent spots in boundary layers can be reconstructed qualitatively from the average behaviour of macroscopic measures in the transition zone. The conclusion in [1] that there exists a connection between the patterns in laminar instability and the birth of turbulent spots is strengthened. We examine why the relationship between instability and transition to turbulence is manifest in some cases and appears to be totally absent in others. Novel cellular automaton-type simulations of the transition zone are conducted, and the pattern of spot birth is obtained from secondary instability analysis. The validity of the hypothesis of concentrated breakdown, according to which most turbulent spots originate at a particular streamwise location, is assessed. The predictions made lend themselves to straightforward experimental verification.

Keywords: Turbulent spots; Instability; Boundary layer

1. Introduction

The physics of the transition to turbulence in a boundary layer has been the subject of a large number of theoretical and experimental investigations. While most of the process is understood, as shown in the schematic picture in figure 1, there are still gaps in our knowledge, as we shall discuss below.

The process begins with the linear amplification of two-dimensional disturbance waves of a narrow band of frequencies. Once the disturbance modes have grown to a certain amplitude, they destabilise three-dimensional secondary modes [2–4]. These modes display a locally regular pattern of maxima, which may be aligned (harmonic) or staggered (subharmonic). Further downstream, in what is termed the transition zone, turbulent spots, or concentrated patches of turbulence, are found, surrounded by quiet laminar flow. The spots grow as they convect downstream, and merge with each other to make the flow asymptotically fully turbulent. Our interest here is in the breakdown of instability waves into turbulent spots. We do not explain the complex physics occurring between the zone of secondary instability and the region containing spots, but we present evidence showing that the pattern existing in the first is retained for the most part in the second.

It is at present almost impossible, either experimentally or numerically to track the birth and downstream growth of a large number of individual turbulent spots and to obtain detailed statistics. It is however not difficult to measure average quantities such as turbulent

*Corresponding author. E-mail: nvinod@jncasr.ac.in or rama@jncasr.ac.in

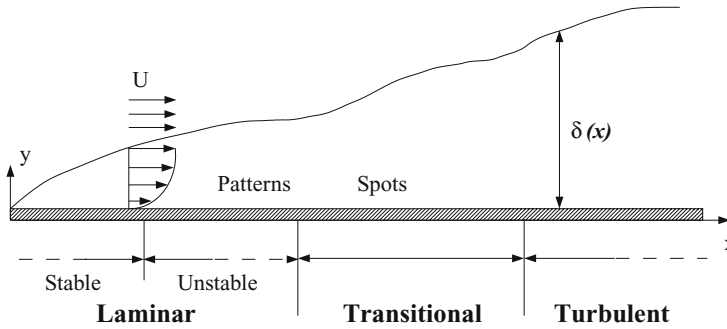


Figure 1. Sequence of events in the laminar-turbulent transition process, on a boundary layer formed by the flow past a semi-infinite plate.

intermittency (the fraction of time that a flow is turbulent). With these, and knowing the behaviour of a typical spot, we demonstrate that it is possible to reconstruct the scenario of spot birth. It was recently shown [1] that intermittency behaviour in many flows is consistent with spot birth as dictated by the most unstable secondary mode. Evidence for this was given for (i) adverse pressure gradient boundary layers in quiet flows and (ii) zero pressure gradient boundary layers in noisy conditions, where streak breakdown occurs. In the present paper, the conclusion that secondary instability is the driver for spot formation according to a spatial and temporal pattern is strengthened. An important question that was left unanswered in the earlier work was that if there is a pattern in spot formation, then why is it that in quiet zero pressure gradient boundary layers, measurements for intermittency match closely with what is expected from a completely random birth of spots. (Since most intermittency measurements have been made for this specific flow, the assumption of random spot birth has gained credence and was not re-examined until [1].) We show here that in this special case, the intermittency variation obtained from both random and regular spot birth are similar, and discuss why. We then present other measures which even in this case would differentiate clearly between random and regular spot birth. We also examine the validity of the hypothesis of concentrated breakdown [5], a crucial assumption made by most researchers during the last several decades, including in the earlier paper. Another interesting phenomenon, noticed repeatedly in experiment, is that the region immediately behind a spot is very unlikely to be turbulent. The effect of this calmed region is studied too. We then exploit the versatility of our simulation method to demonstrate (section 7) that the effect of geometry (in the form of transverse curvature) is significant in the boundary layers on cylinders. It is hoped that the present predictions will motivate experimental efforts.

We conduct secondary instability computations in the standard manner (section 2.), and employ novel cellular automaton type stochastic simulations for spot birth, growth and convection, as described in section 3. We make a number of assumptions. First, while the secondary instability analysis is three dimensional, the stochastic simulations are conducted in a plane parallel to the solid body, when viewed from above. This means that the variations within the boundary layer in a direction y normal to the wall are averaged over. The x - y profile of turbulent spots is not uniform, but given that they are flat objects and the boundary layer thickness is very small ($O(R^{-1})$) compared to the other dimensions), averaging over y is a valid approximation. Second, we employ the hypothesis of concentrated breakdown, according to which all spots are born at a particular streamwise location [5], i.e., at a particular Reynolds number. We show in section 6 that this is a reasonable assumption. We also make use of the experimentally and numerically observed shape and downstream behaviour of single spots, especially the fact that spot growth is self-similar at any pressure gradient.

A spatial pattern in turbulent flows in the form of spirals and spots is observed in the experiments of Prigent *et al.* [6] in plane Couette flow and Taylor–Couette flow. They found that the spatial modulation of turbulent intensity obeys the dynamics of coupled amplitude (Ginzburg–Landau-type) equations with noise.

The present work is confined to the case of low-freestream disturbances, i.e., when the linear and secondary instability route is likely to dominate. In the context of earlier work, we note in passing that the simulations of [7, 8] of bypass transition in boundary layers show that structures such as low-speed streaks in the unstable laminar region could sometimes be precursors of turbulent spots. More recently [9], it is shown, again from direct numerical simulations of bypass transition, that not only instabilities of the strong shear layers associated with streaks, but also streak interaction, which can be quite strong, are spot precursors. Incidentally, at higher levels of freestream disturbance, our earlier simulations [1] match well with the experimental results [10] in bypass transition.

2. Secondary instabilities

At some streamwise location in the boundary layer, small (linear) perturbations begin to grow. When these linear modes have grown to a significant amplitude (of the order of a percent of the mean flow), the new flow becomes unstable to secondary, typically three-dimensional disturbances. The linearised equations describing the secondary instability are obtained by the same procedure as in [11, 12], and describe an eigenvalue problem. Note that secondary instabilities account for one contribution to nonlinearity, that of the triad interaction between the primary Tollmien–Schlichting mode and two three-dimensional disturbances, the sum of whose wave-numbers equals that of the primary.

A Chebyshev spectral collocation method is used for the numerical solution [13]. A grid stretching given by

$$y_j = \frac{b(1 + Y_j)}{1 + 2b/y_\infty - Y_j} \quad (1)$$

is applied, where

$$Y_j = \cos\left(\frac{\pi j}{N_g}\right), \quad j = 0, 1, 2, \dots, N_g, \quad (2)$$

are Chebyshev collocation points. We thus transform the computational domain from $(-1, 1)$ to $(0, y_\infty)$, where y_∞ is chosen to be at least five times the boundary layer thickness, and cluster grid points close to the wall by tuning the parameter b . On changing the computational domain to 10 times the boundary layer thickness, the results changed only in the eighth decimal place. On changing the number of grid points N_g from 80 to 160, the eigenvalues remained identical up to the sixth decimal place. Results for the boundary layer over a zero pressure gradient boundary layer compare very well with those of [11].

We are interested here in the flow past flat solid surfaces inclined at an angle $2m/(m+1)$ to the flow, where the external flow velocity varies downstream as $U_\infty \sim x^m$ [14]. We consider constant pressure ($m = 0$) and decelerating boundary layers ($m < 0$) in this paper, since the behaviour in the transition zone differs in the two. The profile of mean streamwise velocity for a given m is described by the Falkner–Skan equation [15]

$$f''' + ff'' + \frac{2m}{m+1}(1 - f^2) = 0, \quad (3)$$

where $U = f'$. The boundary conditions are $f = f' = 0$ at the wall, and $f' \rightarrow 1$ as $y \rightarrow \infty$. The Falkner–Skan equation is solved using a 4th order Runge–Kutta scheme; the second derivative at the wall is iterated for by a Newton–Raphson method.

Computations have been carried out for a variety of Reynolds number, pressure gradients and the disturbance amplitude A_p of the primary perturbation. The subharmonic mode, of a streamwise wavenumber equal to half that of the primary, is always found to be the most unstable.

3. The transition zone

The transition zone is easiest to describe quantitatively in terms of the variation with the streamwise coordinate, x , of the intermittency, γ which is defined as the fraction of time that a flow is turbulent. Given that the Reynolds number $R(x)$ is the only parameter in the instability problem, it is reasonable to assume that most turbulent spots will originate within a narrow spanwise strip around a particular streamwise location x_t , denoted here as the location of transition onset. This hypothesis of concentrated breakdown [5] is discussed further below. The average rate of spot birth per unit time per unit spanwise distance is denoted by a parameter n . In the case of a random breakdown, the rate of spot creation obeys a Poisson distribution of mean n per spanwise distance. A Poisson distribution in time is appropriate since the probability of spot formation at a given grid location at a given instant of time is very low. In the spanwise coordinate z , the distribution of spot-birth locations is uniform. Under these conditions, γ would vary downstream as [5]

$$\gamma = 1 - \exp\left[\frac{-n\sigma}{U_\infty}(x - x_t)^2\right], \quad (4)$$

or

$$F \equiv \sqrt{-\log(1 - \gamma)} = \sqrt{\frac{n\sigma}{U_\infty}}(x - x_t) \quad (5)$$

such that the intermittency parameter F varies linearly in x . Here U_∞ is the free-stream velocity. The non-dimensional spot propagation parameter σ is related to the geometry of the spot and its downstream growth and convection and is defined [16] as

$$\sigma = \left[\frac{1}{U_r} - \frac{1}{U_h}\right]U_\infty \tan \zeta, \quad (6)$$

where ζ is the angle subtended by the spot at its origin and U_h and U_r , respectively, are the speeds with which its head and rear convect. Such a definition is made possible by large amounts of experimental evidence that the shape and downstream growth of turbulent spots is similar in all pressure gradients: a turbulent spot maintains an arrowhead shape when viewed from above, and, more important, remains self-similar as it grows and convects [16, 17].

It is relatively straightforward to measure other average transition zone quantities such as the burst rate and the persistence time distribution of laminar or turbulent flow as functions of the streamwise distance. The burst rate B is here defined as the mean number of switches from laminar to turbulent flow per unit time at a given location, and the persistence time W of laminar flow is the duration of time for which the flow remains continuously laminar at a given location. The transitional intermittency has been measured in many experiments, but there are no data available for the other measures, as far as we know. It is our suggestion that a lot of information can be gained from knowing how these quantities vary in the streamwise

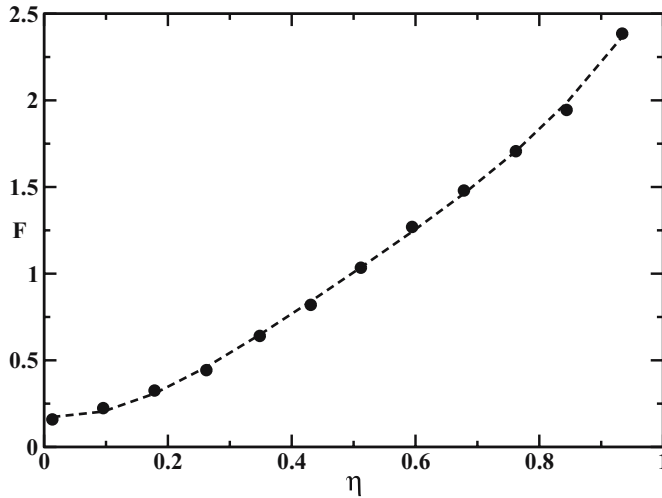


Figure 2. Experimental [30] variation of the intermittency parameter F in adverse pressure gradient, $m = -0.05$. The dashed line is a polynomial fit of the data, showing that F is a nonlinear function of the streamwise distance. The x -axis is scaled, to conform with the manner in which the experimental results are made available, by the streamwise distance where $\gamma = 0.99$.

direction. For a Poisson process, the burst rate is related to the local intermittency by

$$B \propto (1 - \gamma)(-\ln(1 - \gamma))^{1/2}, \quad (7)$$

and the probability density function of persistence time W of laminar flow is

$$p(W) \propto (1 - \gamma)^{W-1}(-\ln(1 - \gamma)). \quad (8)$$

In quiet facilities, the parameter F in equation (5) in constant pressure flow (to be discussed later) varies almost perfectly linearly with x , but its variation in decelerating flows is nonlinear with an increasing slope, as seen in figure 2. The explanation [1] for the nonlinear behaviour of intermittency is that spot birth is not random, but mainly regular, in a pattern dictated by the most unstable secondary mode.

4. Stochastic simulations

Stochastic simulations of the transition zone (using a cellular automaton-like approach) are performed, employing observed properties of spot growth and convection [1, 18]. The simulations are carried out in a similar to those of [19]. We consider two scenarios for spot birth. The first is a random breakdown, as discussed above, with no relation to instability. The second is predominantly regular breakdown, where the pattern prescribed is that of the maxima in disturbance vorticity in the secondary instability. Simulated transition zones for random and regular (subharmonic) breakdown are shown schematically in figures 3 and 4, respectively. A similar figure for harmonic breakdown is available in [1].

The zone, as viewed from above, is discretised into $L_x \times L_z$ rectangular grids in x and z . For most of the simulations it was sufficient to use $L_x = 200$ and $L_z = 400$. Each grid is assigned an integer χ , equal to 0 if the flow there is laminar and 1 if it is turbulent. A regular breakdown scenario is prescribed as follows. During the first time interval, one spot is generated every N_z sites, at $X = 1$ and $Z = lN_z + i$, $l = 0, 1, 2, \dots, L_z/N_z$, where i is an integer between 1

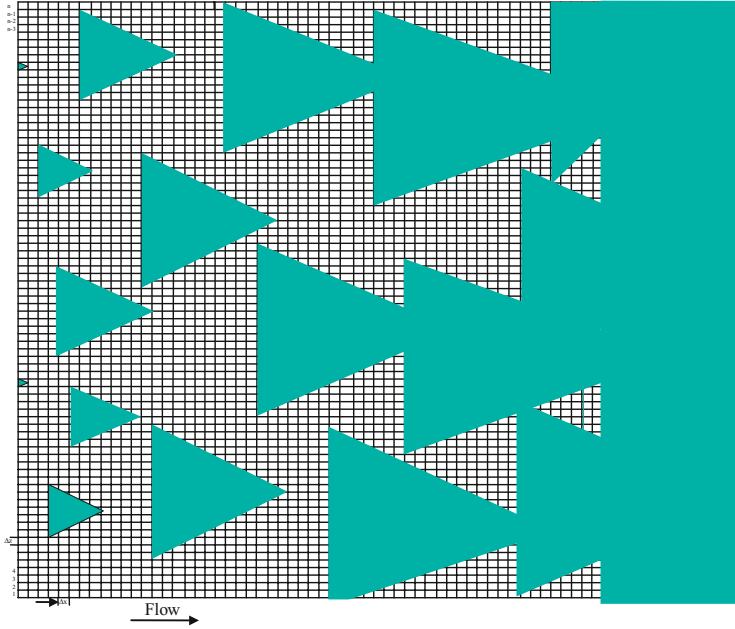


Figure 3. Schematic diagram of the simulation domain in a random spot breakdown scenario. Spots appear according to a Poisson distribution in time, and are uniformly distributed in the spanwise direction.

and N_z . The uppercase stands for discretised coordinates. After N_t time steps the spots form at spanwise locations which are staggered in the spanwise coordinate with respect to the spots generated earlier, i.e., at $X = 1$ and $Z = lN_z + j$ for harmonic and $Z = (l + 1/2)N_z + j$ for subharmonic breakdown, where $j = i + 1$. This prescription corresponds to spots forming at

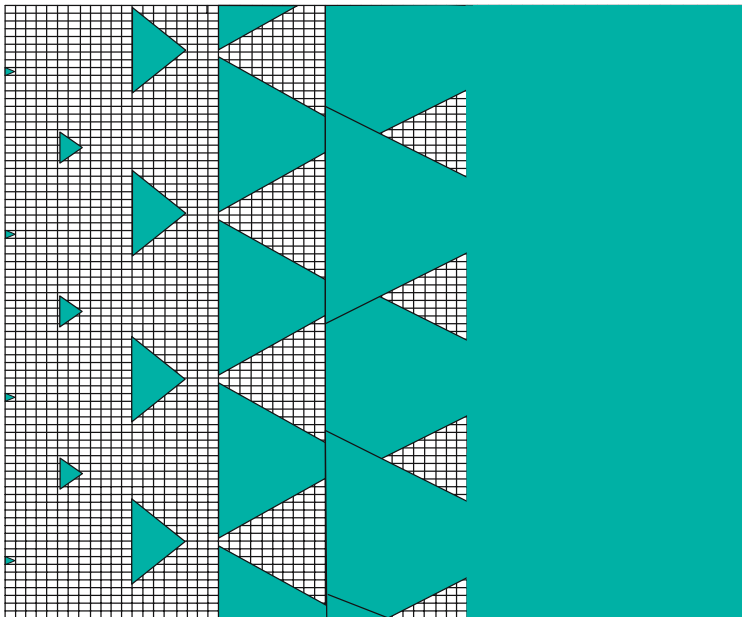


Figure 4. Schematic diagram of the simulation domain in regular breakdown (subharmonic). Spots are formed at regular intervals in the spanwise direction and are staggered after every time period, in a manner dictated by the secondary instability.

the crests of an oblique wave of spanwise and streamwise wavenumbers

$$\beta = \frac{2\pi}{N_z \Delta Z} \quad \text{and} \quad k = \frac{2\pi}{N_t \Delta T v}, \quad (9)$$

respectively, where v is the streamwise velocity of the wave crest. ΔT and ΔZ are the spacing between two consecutive spots in time (T) and spanwise coordinate (Z), respectively. At a given pressure gradient, two pieces of information come from the secondary stability analysis: (1) which kind of breakdown is dominant, and (2) what is the ratio of spanwise to streamwise spacing between consecutive rows of spots. The answer to the first is that we find always the subharmonic to be dominant at the levels of disturbance amplitude we have considered. However, the stochastic simulations are equipped for both types of breakdown. The second quantity is the ratio N_z/N_t , obtained from equation (9), using the wavenumbers k and β of the most unstable secondary mode. The phase of the oblique wave is randomised with a small probability (1%), and a small fraction (5%) of the spots are generated randomly. It is assumed that this prescription mimics qualitatively the randomisation due to external disturbance. Changes in these fractions do not change the answers significantly.

In a random breakdown, spots appear at $X = 1$ in accordance with a Poisson distribution in time and a uniform distribution in the spanwise direction as discussed above. In each case, the downstream growth of turbulent spots follows the same algorithm. During one time interval, the front of each spot moves ahead by two grid locations, while the rear moves forward by one grid location. The lateral dimension of the spot is increased by one grid location on either side. The simulated spot is thus triangular, and retains its shape for all time. A real spot is blunter at its leading edge than a triangle, but this is assumed not to change the results significantly.

In experiments, the speed of the front of the spot is comparable to the flow velocity U_∞ while the rear moves forward approximately at $0.5 U_\infty$. The half-angle ζ subtended by the spot at its origin is about 10° in a constant pressure boundary layer, and increases with adverse pressure gradient.

In the early part of the transition zone, when the individual spots are very much smaller than the lateral extent of the computational domain, one could use either periodic boundary conditions in the lateral direction, or outflow boundary conditions, and the answers would remain the same. If the lateral extent were to become comparable to an individual spot size, periodic boundary conditions would be incorrect in two dimensions, since the spot would begin to wrap around itself. A lateral extent of the computational domain much greater than the base of a spot is used, and it is checked that either lateral boundary condition above gives comparable results. With outflow boundary conditions, we take the precaution of neglecting, for the purpose of obtaining statistics, a large enough lateral region on each edge of the span. The L_z value quoted is after ignoring this lateral portion, and statistics are typically collected in the middle of this region.

In figures 5 and 6 it is demonstrated that intermittency behaviour is sensitive to the ratio of spanwise to streamwise wavenumbers. This observation is used to strengthen the connection we make between instability and its signature in the transition zone. The simulations shown in figure 5 display a distinct change in slope at $X = 13$, just downstream of the location ($X = 11$) at which the heads of a set of spots formed at a time T just touch the rears of the spots formed at $T - N_t \Delta T$. In the simulations of figure 6, all parameters have been kept the same, except that the values of N_z and N_t have been switched. In this case the spots touch each other laterally first (at $X = 6$) downstream of which a sharp change in slope is again evident. At low F , i.e., upstream of spot merger, the intermittency behaviour in each case is exactly the same as that when spots form randomly (with the same breakdown rate). This is not surprising, given that the spots are too small to 'see' each other. At higher intermittencies, quite surprisingly, for the same mean breakdown rate and identical spot growth, the length of the transition zone is seen

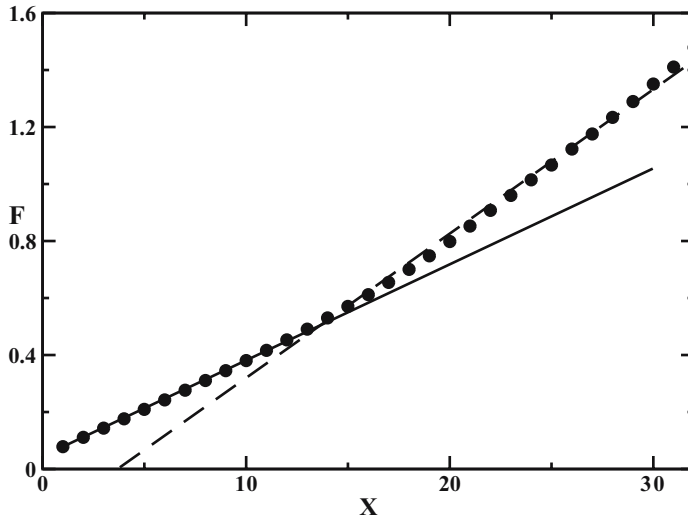


Figure 5. Streamwise variation of the intermittency parameter for $N_z = 49$ and $N_l = 10$. Symbols: regular breakdown, solid line: random breakdown. The mean spot generation rate is kept constant at $n = 0.01$. The dashed line shows the best linear fit for the downstream part of F .

to be very different, which tells us that spot merger plays a large role in transition. A purely lateral merger results in a much higher degree of overlap (on both sides), and consequently, less of the region is occupied by spots. This of course means that transition to turbulence will proceed much more slowly as shown in figure 6. A purely longitudinal merger on the other hand, results in far less spot overlap, meaning more occupancy by spots, and a shortened transition zone (figure 5). Incidentally, it is often the case that experimental results seem to lie on two straight lines, as in this figure. This has been termed a ‘sub-transition’ [20]. Our

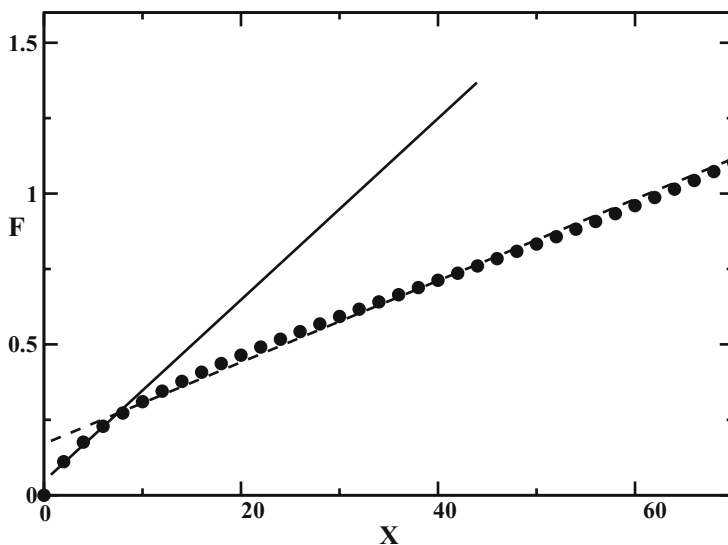


Figure 6. Streamwise variation of the intermittency parameter for $N_z = 10$ and $N_l = 49$. Other parameters and notation are the same as in figure 5. It can be seen that the transition zone is much longer in this case.

simulations show that this change in slope is not a result of spots suddenly changing their downstream growth behaviour, but is a natural consequence of their spatial arrangement.

We now ask which kind of merger scenario would be consistent with growing instability modes. To do this, we perform a secondary instability analysis to obtain the streamwise and spanwise wavenumbers for which the secondary wave grows fastest. For example, for an adverse pressure gradient flow of Falkner–Skan parameter $m = -0.06$, the maximum growth rate (ω_i) of the secondary instability wave is 0.067, and occurs when the wavenumbers (k and β) are 0.165 and 0.215, respectively. The corresponding phase speed is $0.524 U_\infty$. Using the fact that the rear of a spot travels at approximately half the freestream velocity, we have $\tan \zeta = 2\Delta Z/U_\infty \Delta T$. The spot propagation angle is taken as $\approx 20^\circ$, which is close to the experimental value for this pressure gradient [21], and from equation (9), we may estimate the breakdown ratio N_z/N_t to be ~ 4.9 . This ratio changes only by 2% for a 50% change in the Reynolds number, and may be taken to be independent of the Reynolds number.

In figure 7, we consider an adverse pressure gradient, $m = -0.05$. The ratio N_z/N_t obtained from stability analysis for this case is 3.23, and in the stochastic simulations we use $N_z = 39$ and $N_t = 12$. The analysis is done at a Reynolds number of 220, based on the boundary layer momentum thickness, to match the experimental value. A similar result for $m = -0.06$ is available in [1]. The results of both simulations are in good agreement with experiments. In particular, the changing slope of the intermittency parameter $F(x)$ is followed well. We may conclude that a spot breakdown pattern as prescribed by the secondary instability gives rise to intermittency behaviour in qualitative agreement with measurements in highly decelerating flows.

It may be noted that there is some discrepancy at the beginning of the transition zone, where it is known that experimental data may be inaccurate: errors could arise unless the data are collected over extremely long times. Secondly, tiny patches of turbulence can be difficult to distinguish from noise. It is also to be remembered that the hypothesis of concentrated breakdown is an idealisation: in reality spots would be forming within a narrow streamwise

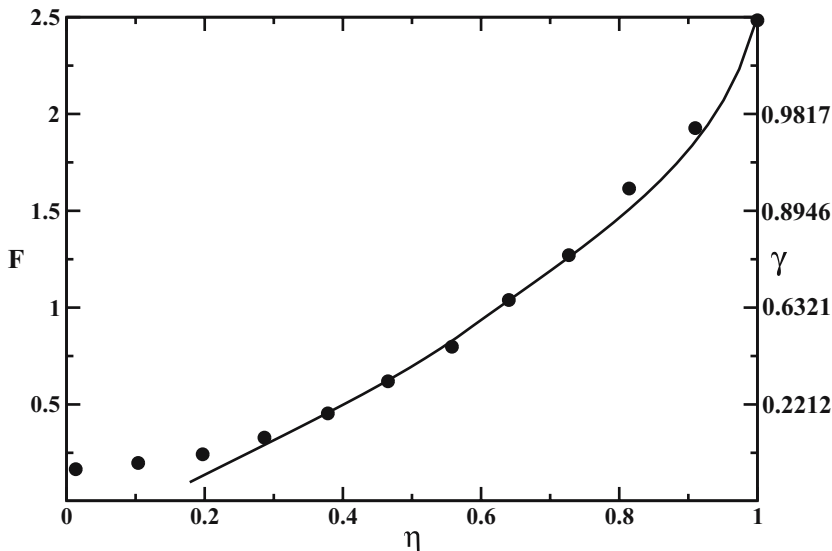


Figure 7. Downstream variation of the intermittency parameter F in an adverse pressure gradient of $m = -0.05$. Solid line: stochastic simulations with $N_z = 39$, $N_t = 12$, from the dominant secondary mode, symbols: experiments [31].

strip around $x = x_t$, rather than at one particular location; this can smear out the intermittency at $\gamma \sim 0$. There are several techniques for distinguishing between laminar and turbulent patches in experiments, which include band-pass filtering and the fixing of thresholds. All of these are subject to error, which are likely to be magnified at small or large intermittency, especially at $\gamma \rightarrow 1$.

The burst rate is discussed in [1]. Its behaviour when the dominant merger is lateral is qualitatively different from the case where the merger is longitudinal.

The probability density function of the persistence time W plotted in figure 15. The data are obtained by running the simulation over 20 million time steps (after reaching stationary state), monitoring a particular streamwise location in the middle of the span and collecting statistics of lengths of strings of zeroes between two 1's. At low values of intermittency, the persistence time of turbulent patches is just a triangular function, emerging from the size and shape of an individual spot. On the other hand, the strings of zeroes give more information about the gaps between turbulent patches, which is a function of both the rate and spatial distribution of spot formation, as well as the merger scenario. The reverse information about strings of 1's between two zeroes is less interesting. (At low intermittency levels, this quantity only tells us about the streamwise size of a spot.) We present results for W at a location where the intermittency is $\gamma = 0.1$. For a random spot breakdown, the probability density of the persistence time decays exponentially with persistence time, as is expected from equation (8). At low intermittency levels, in the case of regular breakdown with dominant longitudinal merger, an overall decay is significantly modulated by ups and downs ([1] and seen later in figure 15). The most probable persistence times correspond to the modulated streamwise extent of the laminar zone between two rows of spots. In harmonic breakdown, the biggest peak is at the spacing corresponding to the row of spots immediately behind the present one; the second peak is at the value corresponding to two rows behind. The probability of W between these values, and their multiples, will be lower. Since the leading edge of the spot is not flat, there will be smooth oscillations, not sharp rises and falls. The picture is similar in

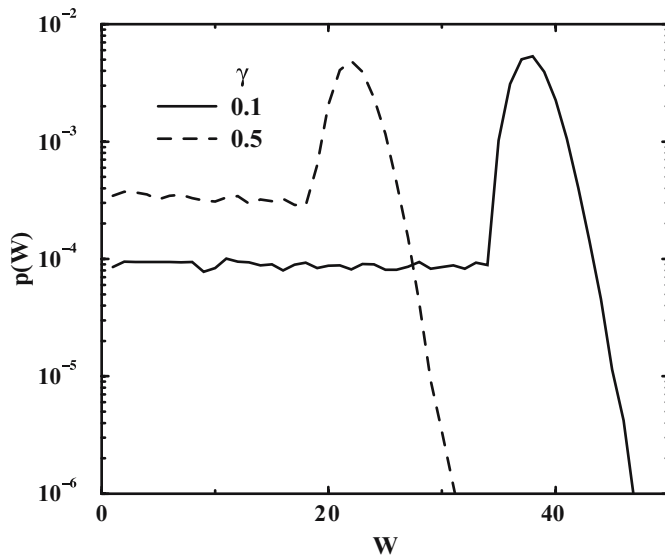


Figure 8. Probability density function of persistence time of laminar flow at $\gamma = 0.1$ (solid line) and $\gamma = 0.5$ (dashed line). The simulations are carried out under conditions where lateral merger is dominant as in figure 6. The parameters chosen for the simulations are $N_t = 4.9$ and $N_z = 10$.

subharmonic breakdown, but in predominantly longitudinal merger, we expect the second row of spots (the aligned ones) and not the first row (staggered ones) to give the highest peak, as the simulations bear out. At higher levels of intermittency, if the breakdown is predominantly regular, the probability of very large waiting times is extremely low, as expected. In the reverse case, of predominantly lateral merger, we mainly have patches of turbulence separated by a serrated laminar region, so we expect a single peak with a gradual fall on either side of it. The location of the peak is at a higher W (larger waiting time) for a lower intermittency. In figure 8 the probability density function of the persistence time for this case is plotted. The qualitative behaviour, as expected, is different from a predominantly longitudinal merger scenario, and an experimental measurement of $p(W)$ can thus indicate the dominant breakdown pattern.

5. Is spot birth random in constant pressure gradient flows?

In constant pressure flow, two kinds of behaviour are observed. In high-disturbance environments, the intermittency behaviour is similar to that seen in adverse pressure gradients, except the dominant mechanism is the secondary instability of streaks. The experimentally measured intermittency in such a flow [10] has been shown [1] to be consistent with the dominant instability pattern. Most experiments, however, are conducted on a zero pressure gradient boundary layer in environments which are maintained quiet. Here, the intermittency parameter F is linear in x , consistent with random spot-birth. Do secondary instabilities not directly trigger spot birth here? A partial answer may be gleaned from figure 9, where the spanwise/streamwise ratio of wavelengths of the dominant mode is shown as a function of the pressure gradient. The ratio decreases with decreasing pressure gradient, and N_z/N_t is about 2.3 for a constant pressure boundary layer (since now $k = 0.085$, $\beta = 0.146$ and $\nu = 0.353$ for the most dangerous mode). For a regular breakdown with this ratio, results of the simulations

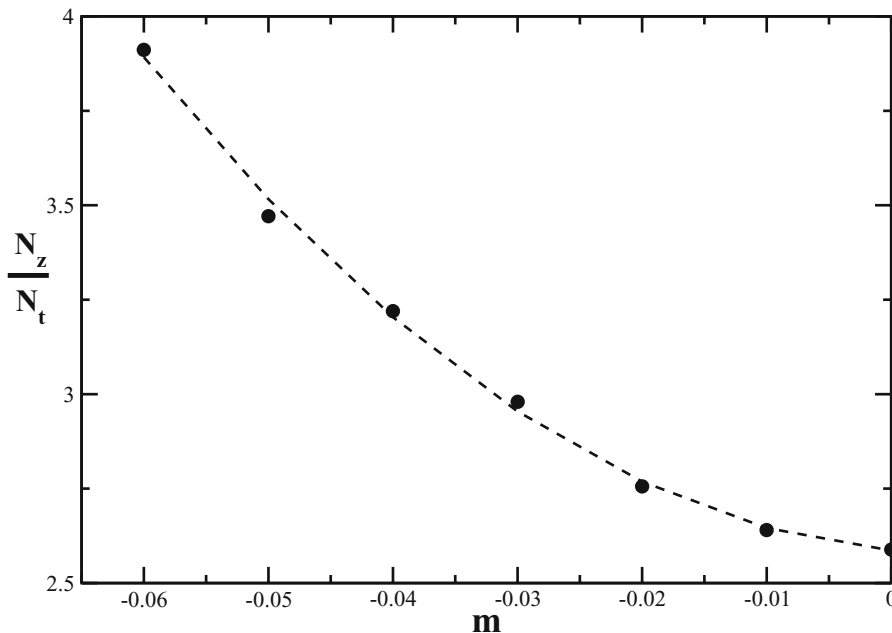


Figure 9. The variation with pressure gradient of the ratio N_z/N_t , as determined by the most unstable secondary mode.

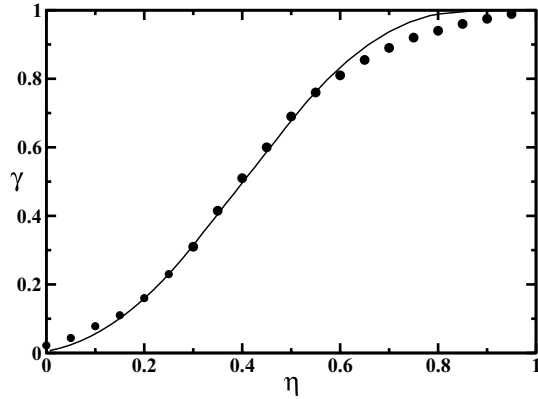


Figure 10. Variation of γ in the boundary layer over a flat plate. Solid line: stochastic simulations with $N_z = 32$, $N_t = 13$ as dictated by secondary instability, the dots are experimental data in constant pressure boundary layers [32].

agree well with experiments up to high levels of intermittency (see figure 10). In the corresponding intermittency parameter plot in figure 11 it is seen that the variation in F is linear up to about $\gamma = 0.75$ (figure 11). The slope increases towards the end of the transition zone. On the lines of the discussion on figures 5 and 6, we may expect that spot mergers are now a combination of lateral and longitudinal, with longitudinal being marginally dominant. The weakened dominance means that the slope change occurs much closer to full turbulence, at $\gamma \sim 0.8$. The difference at high intermittency in the F is seen to be almost nonexistent when we look at the same data in terms of γ . This is because, from equation (5), when $\gamma \rightarrow 1$, the variation in F is very sensitive to the value of γ . Since experimental results at high γ are not very accurate, as discussed earlier, we do not lay too much emphasis on this region.

The obliqueness of the most unstable wave is the major reason for why the variation in F is much less nonlinear for zero pressure gradient flows. However, this may not provide the complete answer for why the variation of F is linear. The perfectness of the linear fit in a vast number of experimental data may also be because the degree of randomness in this case is

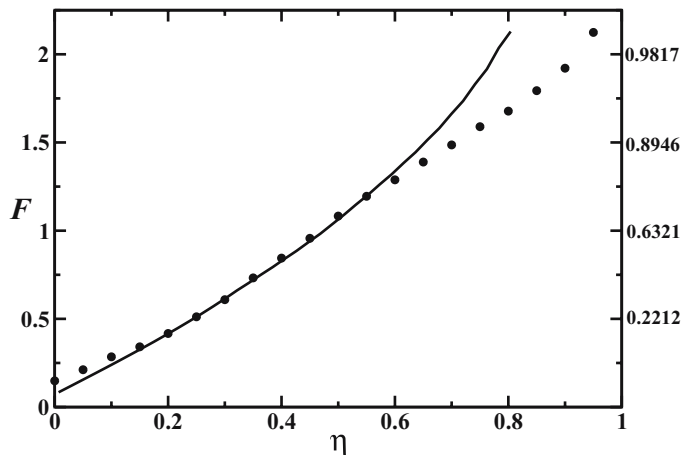


Figure 11. The variation of intermittency parameter F in the boundary layer. Simulation parameter is same as figure 10.

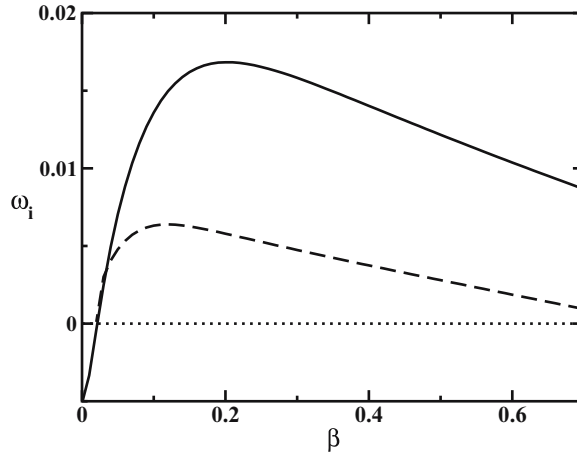


Figure 12. The growth rate of most dangerous secondary sub-harmonic mode at a Reynolds number $R = 600$, based on the momentum thickness of the boundary layer and U_∞ . Solid line: $m = -0.06$, $k_+ = 0.14$, dashed line: $m = 0$, $k_+ = 0.085$.

actually higher than in an adverse pressure gradient boundary layer, as suggested by Gostelow and Walker [22]. The following qualitative arguments indicate why we may expect this.

A decelerating flow is inherently much more unstable [23, 24], as demonstrated in figures 12 and 13. Since the primary wave is slowly growing, we assume that the secondary mode at a given time can be computed by taking the primary wave to be of constant amplitude (this is a temporal analogue of the ‘parallel-flow’ assumption often employed in spatially developing flow). It is to be noted that the growth of the secondary mode can be faster

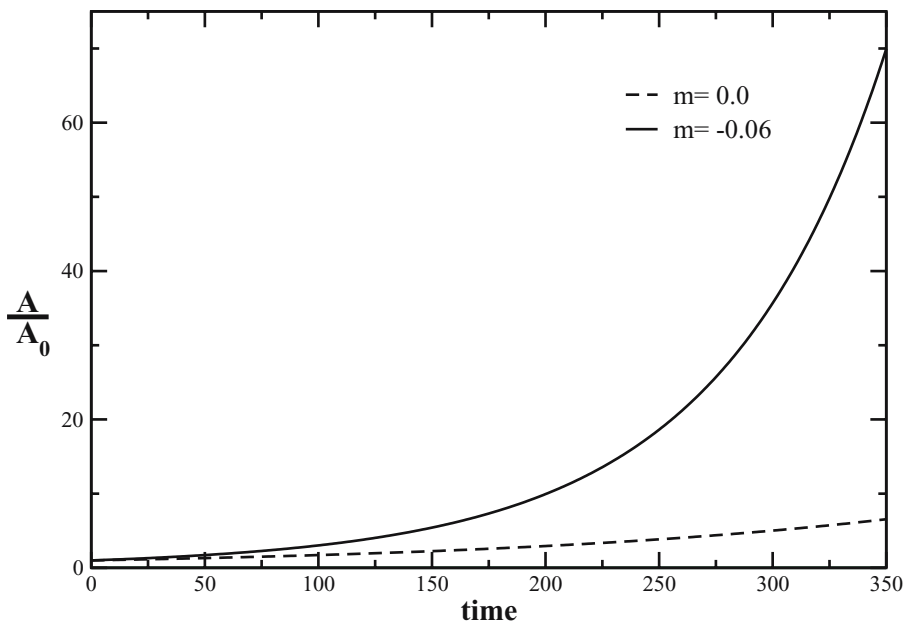


Figure 13. The variation of amplitude of secondary disturbance wave with time in adverse ($m = -0.06$, $k = 0.185$ and $\beta = 0.12$ (solid line)) and zero ($k = 0.13$ and $\beta = 0.805$) pressure gradient boundary layers.

Table 1. Typical phase and group velocities in zero pressure-gradient and decelerating boundary layers.

Pressure gradient (m)	Reynolds number	Phase speed	Group velocity
0	200	0.412	0.295
-0.05	200	0.492	0.655
0	600	0.353	0.188
-0.05	600	0.510	0.666

than exponential if the primary mode is unstable as well. Within a very short downstream distance, the disturbance waves in an adverse pressure gradient flow achieve the threshold amplitude required for breaking down into spots. In the constant pressure case the attainment of the required threshold is much slower, offering greater opportunity for stochastic effects.

A significant amplitude modulation of wave packets could be another cause for randomness in zero pressure gradient flow. Amplitude modulation would result in different waves reaching the threshold at different streamwise stations, and spot birth would be smeared out over a streamwise distance. In the case of decelerating flow, the group velocities of the waves are much larger, as seen in table 1, and the amplitude modulation takes place over a much narrower width. At a Reynolds number of 200, the group velocity c_g of the most unstable secondary instability in adverse pressure gradient is more than twice the corresponding wave in a zero pressure gradient boundary layer. At a Reynolds number of 600, this ratio is more than 3. The phase speeds on the other hand are not that different.

Finally, the wavelength ratio of the dominant mode varies significantly with primary disturbance amplitude in zero pressure gradient boundary layers (see [25]). This, however, is not the case in strongly decelerating flow, as seen in table 2. If the external noise is irregular in amplitude, a greater randomisation would take place in zero pressure gradient flow than in decelerating flow.

These results indicate that in a decelerating boundary layer, formed by the flow past an inclined plate, the connection between instability and transition is likely to be much easier to observe, and we therefore recommend experimental work in adverse pressure gradient, rather than on zero pressure gradient boundary layers.

6. Effect of concentrated breakdown

Narasimha [5] proposed the hypothesis of concentrated breakdown in which all spots form within a narrow spanwise belt around the location of transition onset, i.e., within $x_t \pm \epsilon$,

Table 2. Effect of the primary disturbance amplitude on the obliqueness of the most dangerous mode.

A	R	k_+/β	
		$m = 0.00$	$m = -0.049$
0.01	200	0.77	0.75
0.005	200	0.91	0.70
0.01	600	0.65	0.70
0.005	600	0.81	0.75

where $\epsilon \ll x_t$. While the intermittency behaviour resulting from the hypothesis and the assumption of a random breakdown matches the experiment very well in constant pressure and low-disturbance environments, its validity has been a matter for debate, see e.g. [26]. Since a particular disturbance amplitude is achieved at a particular Reynolds number, it is plausible at least that upstream of a given x location, no spots will form. A large number of spots are likely to form in the vicinity of x_t , but given that instability modes which are not dominant could continue to grow in the transition zone, a small number could be born at any location downstream. We conduct simulations to estimate how much the intermittency and other parameters depend on making this hypothesis. We do this by allowing an increasing fraction of the spots to form with equal probability anywhere downstream of x_t . A random breakdown is prescribed. In time, spots are born as before according to a Poisson distribution at the prescribed rate. This rate is maintained the same for a set of simulations. What is varied is the fraction p of spots that are born at the beginning of the transition zone (at $X = 1$). For a fraction p of the spots (where $p = 1$ in all other sections of this paper), X is set to be 1. For the remaining fraction $(1 - p)$, X is chosen to be anywhere in the domain in the same manner as for Z .

The intermittency distributions for the extreme cases tried are shown in figure 14. It is seen that even when 80% of the spots form downstream of the onset location, the variation of F is still practically linear. However, when all the spots are born downstream of x_t (as modelled by Emmons [27]), there is a notable departure from linearity. In an instability-driven transition, it is highly likely, as discussed above, that a significant fraction of spots will be born around x_t . It may be noted that the intermittency behaviour in the case of Emmons breakdown does not appear very different qualitatively from a regular breakdown, and would thus be difficult to distinguish in an experiment. However, an experiment which measures persistence times can distinguish very simply between them, as is evident from figure 15. In an Emmons breakdown, the persistence time distribution decays exponentially, but with a smaller slope than for the concentrated breakdown, as expected. Our basic conclusion is that even in the unlikely event of a large fraction of spots being born downstream, the intermittency is dominated by spots forming at x_t , since at any given x , these spots are much larger than those born more recently.

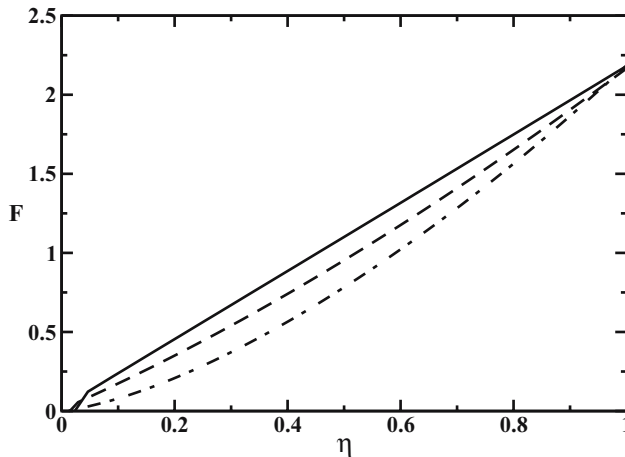


Figure 14. The effect of the hypothesis of concentrated breakdown on the intermittency distribution. Solid line: spots are allowed to form only at x_t . Dashed line: 80% spots are born downstream of the onset location. Dot-dashed line: all spots form downstream of the transition onset (Emmons breakdown).

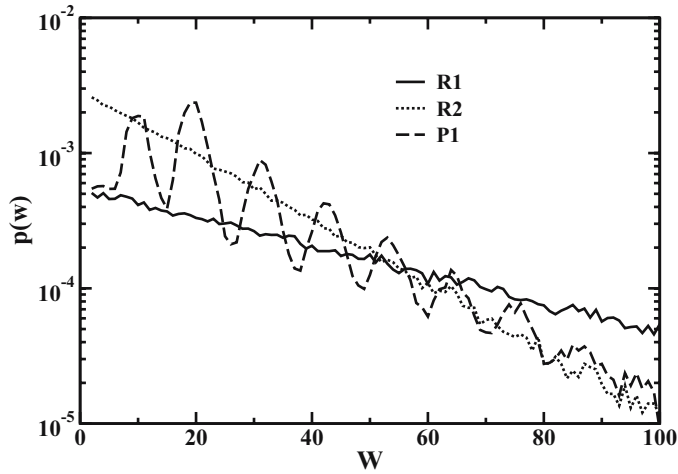


Figure 15. The effect of concentrated breakdown on persistence time distribution. The persistence time is computed at location where intermittency $\gamma = 0.1$. The curve marked R2 is according to the hypothesis of concentrated breakdown, R1 is for random breakdown anywhere downstream of x_t P1 represents periodic breakdown (sub-harmonic), the pattern is obtained from secondary instability.

7. Axisymmetric boundary layers

Transition to turbulence in the boundary layers forming around axisymmetric bodies is poorly understood in spite of wide application in the motion of submarines, fishes etc. When the transverse curvature is significant, transition can proceed quite differently from a two-dimensional boundary layer [20, 28]. When the typical patch of turbulence, consisting either of a single spot or a group of spots which have merged laterally, attains a width of the order of the diameter of the cylinder, it wraps itself around the body. Downstream of the location of wrap, further lateral growth is not possible. The turbulent patch then resembles a sleeve [29] displaying only a one-dimensional growth in the streamwise direction.

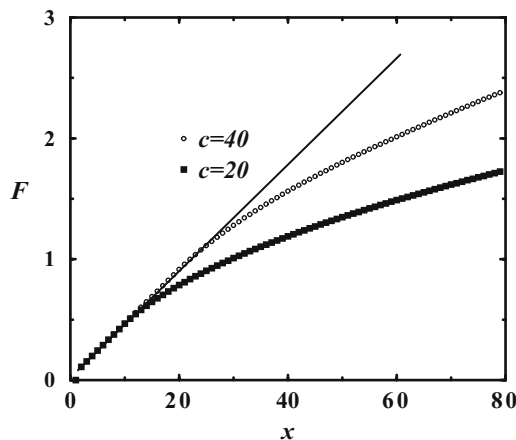


Figure 16. The intermittency factor F versus x , for different circumferences of the cylinder. The straight line is the result of two-dimensional simulations with the same spot birth rate.

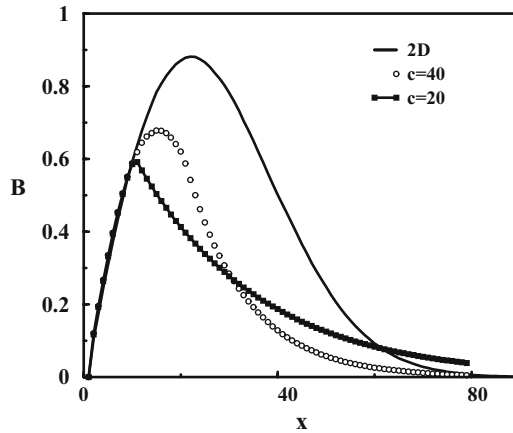


Figure 17. The burst rate in the transition zone of the boundary layer around a cylinder.

We have carried out stochastic simulations of the birth and downstream propagation and growth of turbulent spots in the transition zone of an axisymmetric boundary layer. The downstream variation of the intermittency parameter F is shown in figure 16. The quantity c is the circumference of the body. In the initial region, transition proceeds exactly as it would in two-dimensional flow. This is because spots are too small to “see” the body. When spots wrap themselves around the cylinder, a qualitative change is observed, as is expected from the discussion above, and transition proceeds much more slowly after this. The burst rate B shown in figure 17 is another indication of the differences in the transition process.

8. Summary and discussion

Stochastic simulations, inspired by a cellular-automaton approach, of the generation and propagation of turbulent spots in transitional boundary layers have been conducted, employing the observation that spot growth is self-similar. It is demonstrated that the pattern of spot birth may be inferred from the downstream variation of average quantities in the transition zone, such as the intermittency and the burst rate. This is because the qualitative behaviour in the transition zone depends on whether there is a pattern in spot merger, and if so, whether lateral or longitudinal merger is dominant. Contrary to present belief, our results indicate that relatively simple experiments can tell us a great deal about the connection between instability and transition to turbulence. We show that experiments conducted in decelerating flows are much more conducive to exploring this connection than constant pressure flows. Transverse curvature has the effect of slowing down the transition process.

The simulations of [7] showed a degree of spanwise periodicity in the arrangement of the backward jets (the precursors to spots). Only some of the jets however gave rise to turbulent spots. It has been our contention in TS-mode driven transition that the degree of randomness in the birth of spots is expected to decrease as the pressure gradient becomes increasingly adverse. It would be interesting to see whether this is true of bypass transition as well. A direct numerical simulation of an adverse pressure gradient flow should, if this contention is right, produce turbulent spots from many more of the reverse jets.

Acknowledgements

We are most grateful to Professor Narasimha for suggesting cellular automaton type simulations for the transition zone, and for several discussions. Financial support from the Aeronautical R&D Board, Government of India, is gratefully acknowledged.

References

- [1] Vinod, N. and Govindarajan, R., 2004, Pattern of breakdown of laminar flow into turbulent spots. *Physical Review Letters*, **93**, 114501.
- [2] Bech, K.H., Henningson, D.S. and Henkes, R.A.W.M., 1998, Linear and nonlinear development of localised disturbances in zero and adverse pressure gradient boundary layers. *Physics of Fluids*, **10**(6), 1405–1418.
- [3] Reed, H.L. and Saric, W.S., 1996, Linear stability theory applied to boundary layers. *Annual Reviews of Fluid Mechanics*, **28**, 389–428.
- [4] Saric, W.S., Reed, H.L. and White, E.B., 2003, Stability and transition of three-dimensional boundary layers. *Annual Reviews of Fluid Mechanics*, **35**, 413–440.
- [5] Narasimha, R., 1957, On the distribution of intermittency in the transition region of a boundary layers, *Journal of Aeronautical Sciences*, **24**, 711–712.
- [6] Prigent, A., Grégoire, G., Chaté, H., Dauchot, O. and van Saarloos, W., 2002, Large scale finite wavelength modulation within transition shear flows. *Physical Review Letters*, **89**(1), 014501.
- [7] Jacobs, R.G. and Durbin, P.A., 2001, Simulations of bypass transition. *Journal of Fluid Mechanics*, **428**, 185–212.
- [8] Wu, X., Jacobs, R.G., Hunt, J.C.R. and Durbin, P.A., 1999, Simulation of boundary layer transition induced by periodically passing wakes. *Journal of Fluid Mechanics*, **398**, 109–153.
- [9] Brandt, L., Schlatter, P. and Henningson, D.S., 2004, Transition in boundary layers subject to free-stream turbulence. *Journal of Fluid Mechanics*, **517**, 167–198.
- [10] Matsubara, M. and Alfredsson, P.H., 2001, Disturbance growth in boundary layers subjected to free-stream turbulence. *Journal of Fluid Mechanics*, **430**, 149–168.
- [11] Herbert, T., 1988, Secondary instability of boundary layers. *Annual Reviews Fluid Mechanics*, **20**, 487–526.
- [12] Govindarajan, R., L'vov, V.S., Procaccia, I. and Sameen, A., 2003, Stabilisation of hydrodynamic flows by small viscosity variations. *Physical Review E* **67**, 026310.
- [13] Canuto, C., Hussaini, M.Y., Quarteroni, A. and Zang, T.A., 1987, *Spectral Methods in Fluid Dynamics*. Springer-Verlag, 1st ed.
- [14] Batchelor, G.K., 2000, *An Introduction to Fluid Dynamics*. Cambridge University Press.
- [15] White, F.M., 1991, *Viscous Fluid Flow*, 2nd edn. (New York: McGraw-Hill).
- [16] Narasimha, R., 1985, The laminar-turbulent transition zone in the boundary layer. *Progress in Aerospace Sciences*, **22**, 29–80.
- [17] Seifert, A. and Wignanski, I.J., 1995, On turbulent spots in a laminar boundary layer subjected to a self similar adverse pressure gradient. *Journal of Fluid Mechanics*, **296**, 185–209.
- [18] Vinod, N. and Govindarajan, R., 2005, Instabilities and transition in boundary layers. *Pramana, Journal of Physics*, **64**(3), 323–332.
- [19] Nagel, K. and Paczuski, M., 1995, Emergent traffic jams, *Physical Review E*, **51**(4), 2909–2918.
- [20] Narasimha, R., 1984, Subtransitions in the transition zone. *Proceedings of IUTAM Symposium on Laminar-Turbulent Transition, Novosibirsk*.
- [21] Gostelow, J.P., Melwani, N., and Walker, G.J., 1995, Effect of streamwise pressure gradient on turbulent spot development. *ASME paper 95-GT-303*.
- [22] Walker, G.J. and Gostelow, J.P., 1990, Effect of adverse pressure gradients on the nature and length of the boundary layer. *Transactions of ASME*, **112**, 196–205.
- [23] Corke, T.C. and Gruber, S., 1989, Resonant growth of three-dimensional modes in Falkner–Skan boundary layers with adverse pressure gradients. *Journal of Fluid Mechanics*, **320**, 211–233.
- [24] Liu, C. and Maslowe, S.A., 1999, A numerical investigation of resonant interactions in adverse-pressure-gradient boundary layers. *Journal of Fluid Mechanics*, **378**, 269–289.
- [25] Zelman, M.B. and Maslennikova, I.I., 1993, Tollmien–Schlichting-wave resonant mechanism of subharmonic-type transition. *Journal of Fluid Mechanics*, **252**, 449–478.
- [26] Johnson, M.W. and Fasihfar, A., 1994, Properties of turbulent bursts in transition boundary layers. *International Journal of Heat and Fluid Flow*, **15**(4), 283–290.
- [27] Emmons, H., 1951, The laminar-turbulent transition in a boundary layer—part 1. *Journal of Aeronautical Sciences*, **18**, 490–498.
- [28] Govindarajan, R. and Narasimha, R., 2000, Transition delay by surface heating.: a zonal analysis for axisymmetric bodies. *Journal of Fluid Mechanics*, **418**, 77–100.
- [29] Rao, G.N.V., 1974, Mechanics of transition in an axisymmetric boundary layer on a circular cylinder. *Zeitschrift für Angewandte Mathematik and Physik*, **25**, 63–75.

- [30] Gostelow, J.P. and Blunden, A.R., 1988, Investigations of boundary layer transition in adverse pressure gradient. *33rd ASME International Gas Turbine and Aeroengine Congress, Amsterdam, Netherlands*.
- [31] Gostelow, J.P., Blunden, A.R. and Walker, G.J., 1994, Effects of free-stream turbulence and adverse pressure gradients on boundary layer transition. *Transactions of the ASME Journal of Turbomachinery*, **116**, 392–404.
- [32] Dhawan, S. and Narasimha, R., 1958, Some properties of boundary layer flow during transition from laminar to turbulent motion. *Journal of Fluid Mechanics*, **3**, 418–437.